Int. J. Electrochem. Sci., 9 **(2014)** 6328 - 6351

International Journal of
ELECTROCHEMICAL
SCIENCE
www.electrochemsci.org

Characterization and Electrochemical Preparation of Thin Films of Binary Heavy Metals (Cu-Pb,Cu-Cd,Cu-Zn) from Simulated Chloride Wastewaters

Abbas Hamid Sulaymon[1], *Sawsan A. M. Mohammed*[2], *Ali Hussein Abbar*[3,*]

[1] Environmental Engineering Department, University of Baghdad, Iraq
[2] Chemical Engineering Department, University of Baghdad, Iraq
[3] Chemical Engineering Department, Al-Qadissya University, Iraq
[*]E-mail: aliabbar68@yahoo.com

Received: 27 May 2014 / *Accepted:* 8 July 2014 / *Published:* 25 August 2014

Cu-Pb, Cu-Cd, and Cu-Zn thin films were electrodeposited from a simulated chloride wastewater solution using stainless steel rotating disc electrode. The linear sweep voltammograms of the single metallic ions show that electrodeposition of these ions was under mass transfer control due to the well-defined plateau observed under different rotations. The voltammograms of binary systems elucidate the possibility of selective separation of copper from these binary systems. Currents transients measurements, anodic linear sweep voltammetry (ALSV) and atomic force microscopy (AFM) were used to characterize the electrocryatalization process and morphology of these thin films. ALSV profiles show a differentiation for the dissolution process of individual metals and binary systems. Two peaks of dissolution Cu-Pb film was observed while three and four peaks observed for Cu-Cd and Cu-Zn films respectively indicating different phases have been existed. The model of Scharifker and Hills was used to analyze the current transients and it revealed that Cu-Pb and Cu-Cd electrocrystalization processes are governed by three –dimensional progressive nucleation controlled by diffusion, while Cu-Zn electrocrystallization process starts as a progressive nucleation then switch to instantaneous nucleation process for $t/t_m>3$.AFM images reveal that Cu-Pb film is more roughness than Cu-Cd and Cu-Zn films.

Keywords: Heavy metals, Electrodeposition, Anodic dissolution, Electrocrystalization, Cu-Pb / Cu-Cd / Cu-Zn thin films.

1. INTRODUCTION

Heavy metals are elements having atomic weights between 63.5 and 200.6, and a specific gravity greater than 5.0 [1].They are toxic pollutants and are usually released into the surface and

ground water due to industrial activities like metal plating facilities, mining operations, fertilizer industries, tanneries, batteries, paper industries and pesticides, etc.[2,3]. Unlike organic contaminants, heavy metals are not biodegradable and tend to accumulate in living organisms and many of them are known to be carcinogenic. The toxic heavy metals of particular concern in treatment of industrial wastewaters include zinc, copper, cadmium, and lead. Zinc is a trace element that is essential for human health. It is important for the physiological functions of living tissue and regulates many biochemical processes. However, too much zinc can cause eminent health problems, such as stomach cramps, skin irritations, vomiting, nausea and anemia [4]. Copper does essential work in animal metabolism but the excessive ingestion of copper brings about serious toxicological concerns, such as vomiting, cramps, convulsions, or even death [5]. Cadmium has been classified by U.S. Environmental Protection Agency as a probable human carcinogen. Chronic exposure of cadmium results in kidney dysfunction and high levels of exposure will result in death. Lead can cause central nervous system damage, kidney damage, damage of liver and reproductive system, basic cellular processes and brain functions[6].Faced with more and more stringent regulations, nowadays heavy metals are the environmental priority pollutants and are becoming one of the most serious environmental problems. So these toxic heavy metals should be removed from the wastewater to protect the people and the environment.

Various technologies such as precipitation, adsorption [7, 8], biosorption [3, 9], ion exchange [10, 11], reverse osmosis [12], electrodialysis [13], ion exchange-assisted membrane separation [14-19], and electrochemical methods [20-23] have been employed to remove heavy metals from various effluents. Electrochemical methods have been receiving greater attention in recent years due to the distinctive advantages of environmental compatibility, versatility and safety. Electrochemical methods compete with other conventional technologies including evaporation, precipitation, ion exchange and solvent extraction to offer solutions to the needs of the many industries. Electrochemical methods, however, are uniquely capable of recovering pure metal for recycle.

The literature on heavy metal ions removal from aqueous electrolytes using electrochemical deposition method is extensive [24-39]. Most of those work concerned with the removal efficiency and mass transfer correlations that describe the electrochemical system using different cathode materials and different electrolytes, however little work has been done on the characterization of the deposits from these systems. It is well known that the initial stage of electrodeposition involving nucleation and nuclei growth, determines not only the properties and morphology of the final deposits, but also the electrochemical reaction rate under which the electrochemical removal of heavy metals is proceeded [40]. Also the knowledge of the nucleation and subsequent growth of electrodeposits at the nanometer scale promotes understanding the process as accurately as possible to achieve desired properties and applications ,therefore the characterization of the deposited films is essential for any electrochemical removal process to investigate the morphology and mechanism of formation of such deposits[41].

The characterization and mechanism of electrodeposition of single metals like Cu, Pb, Cd and Zn have been investigated extensively using different electrolytes and cathode materials [42-50].On the other hand references may be found to the simultaneous deposition of Cu-Pb[51,52],Cu-Cd[53-55],Cu-Zn[56-59] however, information on the characterization and basic aspect of the electrochemistry of the these systems are scarcity. Also most of these studies have been achieved from

concentrated solutions with the aid of complexion agents for preparing alloys of special properties. To the best of authors knowledge, no previous work has been conducted to characterization the Cu-Pb, Cu-Cd, and Cu-Zn films electrodeposited from diluted chloride medium using stainless steel as cathode material.

Based on the above consideration, our present work was carried out to prepare and characterize Cu-Pb, Cu-Cd, and Cu-Zn thin films electrodeposited on stainless steel cathode from simulated diluted chloride wastewaters. The choice of stainless steel as cathode material in this study is based on the observation of previous works that stainless steel has been proved to be very effective as a cathode for metal removal from wastewaters[60-63]. This material showed a good stability as cathode and could also be anodically polarized during its regeneration process without damage. Furthermore, stainless steel is an inexpensive material when compared to graphite felt or reticulated vitreous carbon (RVC) which have been extensively used in wastewaters treatment. The binary heavy metals films were electrodeposited and dissolved by a cathodic and anodic linear sweep of electrode potential in the solution containing ions of both metals, NaCl, and boric acid. Another procedure used here was based on potentiostatic transients of current where the dependence between current and experiment time for the formation and growth of a binary heavy metals films at a constant negative potential is recorded. The deposits were characterized by optical and atomic force microscopies.

2. EXPERIMENTAL WORK

The electrochemical experiments were carried out in a conventional three-electrode cell (Pyrex® glass). A homemade 0.0314 cm^2 (316-AISI) stainless steel rotating disc electrode was used as a working electrode. Its surface was polished before each experiment with emery paper of grade 600 (3M). A platinum plate (0.35 cm^2) and a saturated calomel electrode were used as a counter and a reference electrode respectively. Electrochemical experiments were controlled with a potentiostat PGSTAT30 (Autolab), under a computerized control.

Chemicals used here were $CuCl_2.2H_2O$, $PbCl_2$, $CdCl_2$, $ZnCl_2$, NaCl, and boric acid. All of them were reagent grade. The electrolytic solutions were freshly prepared with doubly distill water , the testing containing metallic ions solutions were prepared in such a way that the metallic concentration was around 50mg/l in supporting electrolyte consisting of 0.5M NaCl and 0.1 M H_3BO_3 with final pH of 5 adjusted by using NaOH or HCl. It is important to point out that such solutions were prepared trying to resemble the amount of metallic ions and pH of a typical composition contained in an effluent generated by a plating industry [32].The experiments were performed at 25±1ºC.

All cathodic linear sweep voltammetric experiments were performed at 5 mV s^{-1}, scanning from positive to negative direction. The applied potentials for potentiostatic experiments were determined based on the results of voltammetric experiments. The anodic linear sweep voltammetry (ALSV) experiments were performed in another cell of the same type. In this cell saturated calomel electrode (SCE) also used as a reference electrode. Immediately after the deposition on the RDE, it was washed with extra pure water and transferred into the cell for the ALSV analysis. ALSV analysis was performed in the solution of 0.5M NaCl, 0.1 M H_3BO_3, and pH=5 with a sweep rate of 2mVs^{-1} at

1200rpm. In all cases after the dissolution no traces of the deposit left on the St.St surface were detected, indicating complete dissolution of the deposit. Before each experiment (in the case of deposition and ALSV), the electrolyte was purged with high purity nitrogen (99.999%) for 30 min, while a nitrogen atmosphere was maintained over the solution during the experiment to prevent contamination with oxygen. In the chronoamperometry experiments, series of potential step experiments at different increments were achieved in stationary solution by stepping from open circuit potential to the selected final potentials based on the result of linear sweep voltammograms.

The optical micrographs were obtained using Olympus BX51M with DP70 digital camera system. The AFM analysis was performed using SPM-AA3000 (Angestrom Advanced Inc., USA) in contact mode. AFM images were recorded over scan area (2μmx2μm).

3. RESULTS AND DISCUSSION

3.1. Voltammetric measurements

Figure 1. shows polarization curves corresponding to copper, lead, cadmium and zinc electrodeposited on stainless steel rotating disc electrode for several rotation speeds(400,800,1200,1600,and 2000 rpm). The voltammograms show a limiting current zone in the potential range from -300 to -450 mV vs. SCE for copper, -725 to -900 mV for lead, -900 to -1100 mV for cadmium, and -1160 to -1350 mV for zinc.

One of the most important results are the polarization curves of copper obtained in conditions of the present work. In chloride electrolytes, the reduction of Cu (II) ions occurs in two single electron steps and the reactions can be simplified to the reduction of Cu (II) ions to Cu (I) ions [64]:

$$Cu^{+2} + 2Cl^- + e^- \rightarrow CuCl_2^- \quad (1)$$

Followed by the deposition of metallic copper from the Cu (I) ions, i.e.:

$$CuCl_2^- + e^- \rightarrow Cu^0 + 2Cl^- \quad (2)$$

The overall process for copper deposition from Cu (II) ions then is:

$$Cu^{+2} + 2e^- \rightarrow Cu^0 \quad (3)$$

According to the results of previous works related to the electrodeposition of copper from chloride media, the polarization curve should possess two well plateau regions in stirring solution or two peaks in static solution representing equations (1) and (2) [64].In the present work the reduction of Cu (II) to Cu (I) starts at approximately +220 mV vs. SCE and continue to -250 mV. The relation between current and potential is approximately linear and with no plateau is recognized. The reason may attributed to the lower concentration of Cl^- and higher pH=5 of solution in addition to the using of boric acid in the present work. Previous work shows that $CuCl_2^-$ is not stable at pH higher than 4[65].In addition using vigorous agitation will remove $CuCl_2^-$ from the surface leading to enhancement the reduction of Cu (I) to Cu (II) [66].Using boric acid may be played an important role in the instability of $CuCl_2^-$ by its adsorption on the surface of electrode and maintaining the pH of solution constant during the electrodepostion. Several experimental work indicated that boric acid can adsorb on the electrode and has the property of a surface agent [67-68].

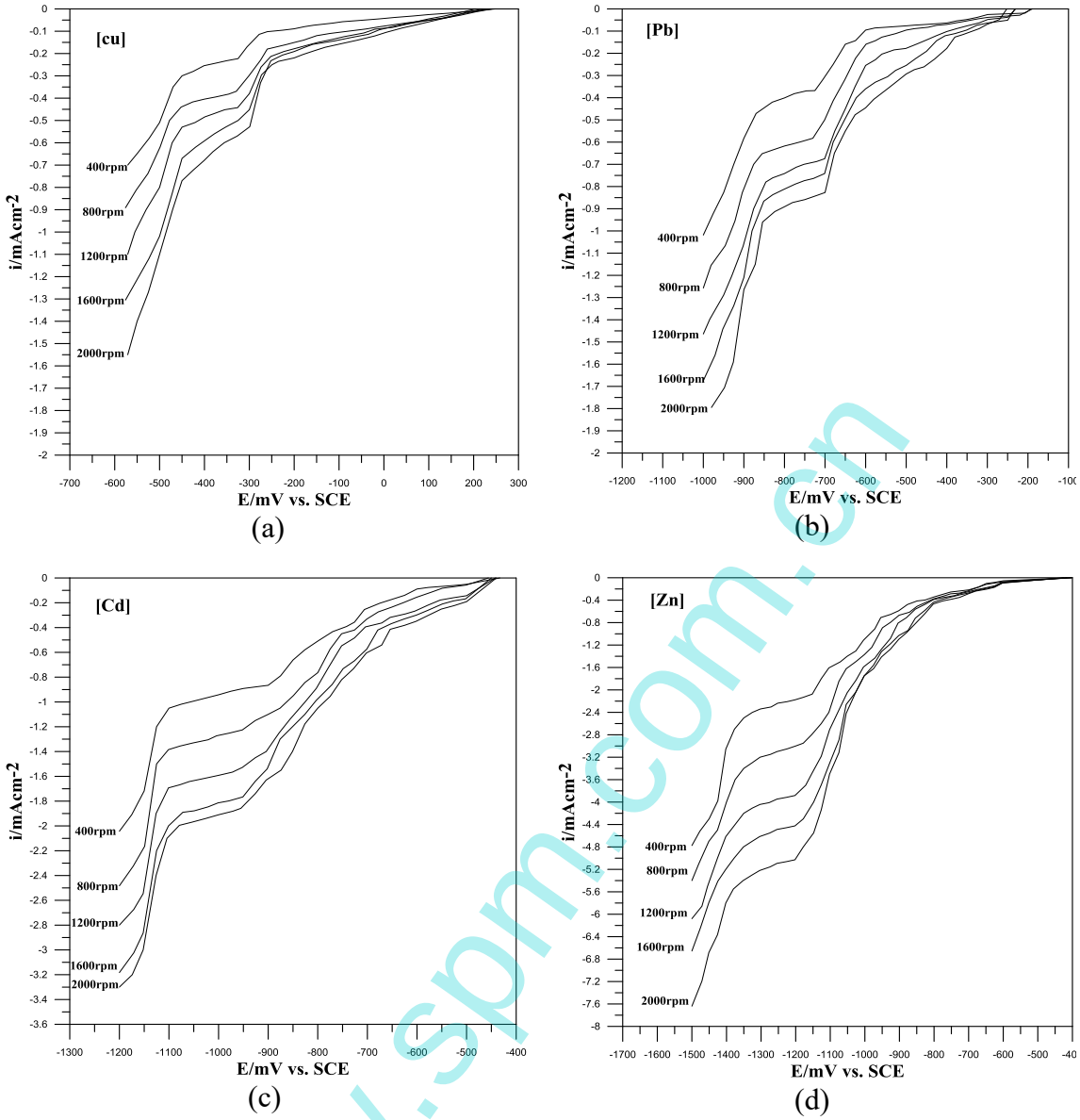

Figure 1. Linear voltammetric curves for reduction of copper (a), lead (b), cadmium(c) and zinc (d) at stainless steel rotating disc electrode at different rotation speeds: [Cu]=[Pb]=[Cd]=[Zn]=50 ppm supporting electrolyte(0.5 M NaCl+0.1M H_3BO_3),pH=5

The reduction of Cu (I), appears at a potential of approximately -300 m V vs. SCE with a well-defined plateau extended to -450 mV vs. SCE. Under such conditions, the reaction rate is limited by the mass transport rate and the limiting current at the smooth rotating disc in laminar flow can be predicted by the Levich equation [69]:

$$I_L = 0.62\, z\, FAD^{2/3}\omega^{1/2}v^{-1/6}c_b \quad (4)$$

Where I_L is the limiting current in mA, A is the area of electrode in cm^2, D is the diffusion coefficient in $cm^2\ s^{-1}$, ω is the rotation rate in rad s^{-1}, ν is the kinematic viscosity of the electrolyte in $cm^2\ s^{-1}$ and c_b is the bulk concentration in $molcm^{-3}$.

To investigate whether the reduction of four heavy metals occurred under mass transfer condition, the limiting currents were calculated from the polarization curves and plotted against $\omega^{1/2}$ as

shown in Figure 2 .The limiting current is found at the middle point of a straight line that follows the plateau region and is limited by E_{max} and E_{min} [70]. These values are the points at which the straight line departs from the I vs. E curve. The results indicate that the reduction of the four heavy metals is under mass transfer control.

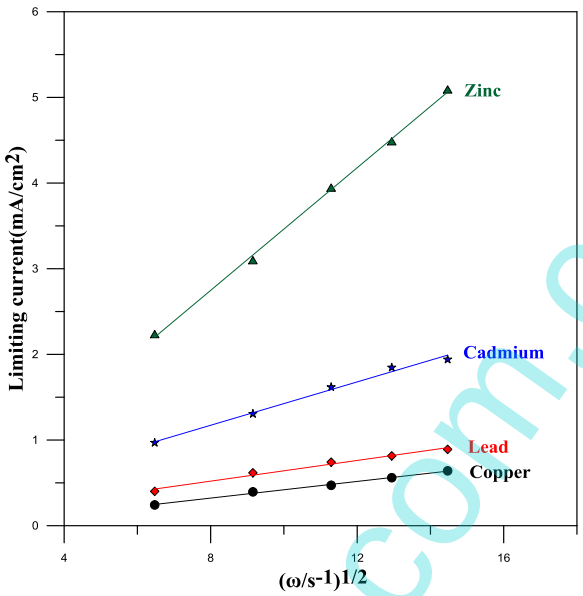

Figure 2. Levich plots for the limiting currents taken at potentials of -380 mV,-790 mV, -1025 mV and -1260 mV vs. SCE for Cu, Pb, Cd, and Zn respectively.

Figure 3. Shows polarization curves for electrodeposition of Cu-Pb, Cu-Cd, and Cu-Zn binary systems from chloride solution at 1200rpm, polarization curves for single metals are also included for comparison. It can be seen that polarization curve of Cu-Pb system starts at more negative potential than single Cu approximately at -73 mV vs. SCE ,the same behavior with respect to Cu-Cd and Cu-Zn binary systems has been observed but at potentials -40 mV and -10 mV vs. SCE respectively. The polarization curves of binary systems are always located between the single metals up to electrode potential -400 mV vs. SCE. At cathode potential more negative than -400 mV vs. SCE the current density of the binary systems is greater than single metals .The cathode potential under which the codepostion of the two metals starts at -500, -700 , and -850 m V vs. SCE for Cu-Pb ,Cu-Cd ,and Cu-Zn systems respectively as observed by increasing the current more rapidly beyond these values of cathode potential.

3.2. Anodic linear sweep voltammetry

Anodic linear sweep voltammetry (ALSV) has been developed as an appropriate in situ technique for electrochemical characterization of the phase composition of thin layers of electrodeposited alloys. This technique is based on the electrochemical principle, that each phase in the coated layer has its own equilibrium potential, i.e. dissolution potential and therefore on the ALSV

each phase should be characterized by its peak of dissolution. For successful application of the ALSV technique appropriate electrolyte should be chosen and low sweep rate of 5-1mVs^{-1} should be applied [71, 72].In the present work, this technique was adapted to obtain more information about the behavior of the binary system of Cu-Pb, Cu-Cd and Cu-Zn electrodeposited under potentiostatic conditions. Therefore, the electrode potential was maintained at-790 mV vs. SCE, -1025 mV and -1260mV for 5 min to form the deposits of Cu-Pb, Cu-Cd and Cu-Zn respectively and then anodic dissolution was carried out using a slow sweep rate (2 mV/s) in the positive direction. The deposition and dissolution steps were achieved at1200rpm.

The ALSV curves of dissolution of single Pb, single Cu, and Cu-Pb binary system are shown in Figure 4.The well separated two anodic peaks, coinciding with those obtained with corresponding single metal deposits, clearly demonstrate the existence of two different phases.

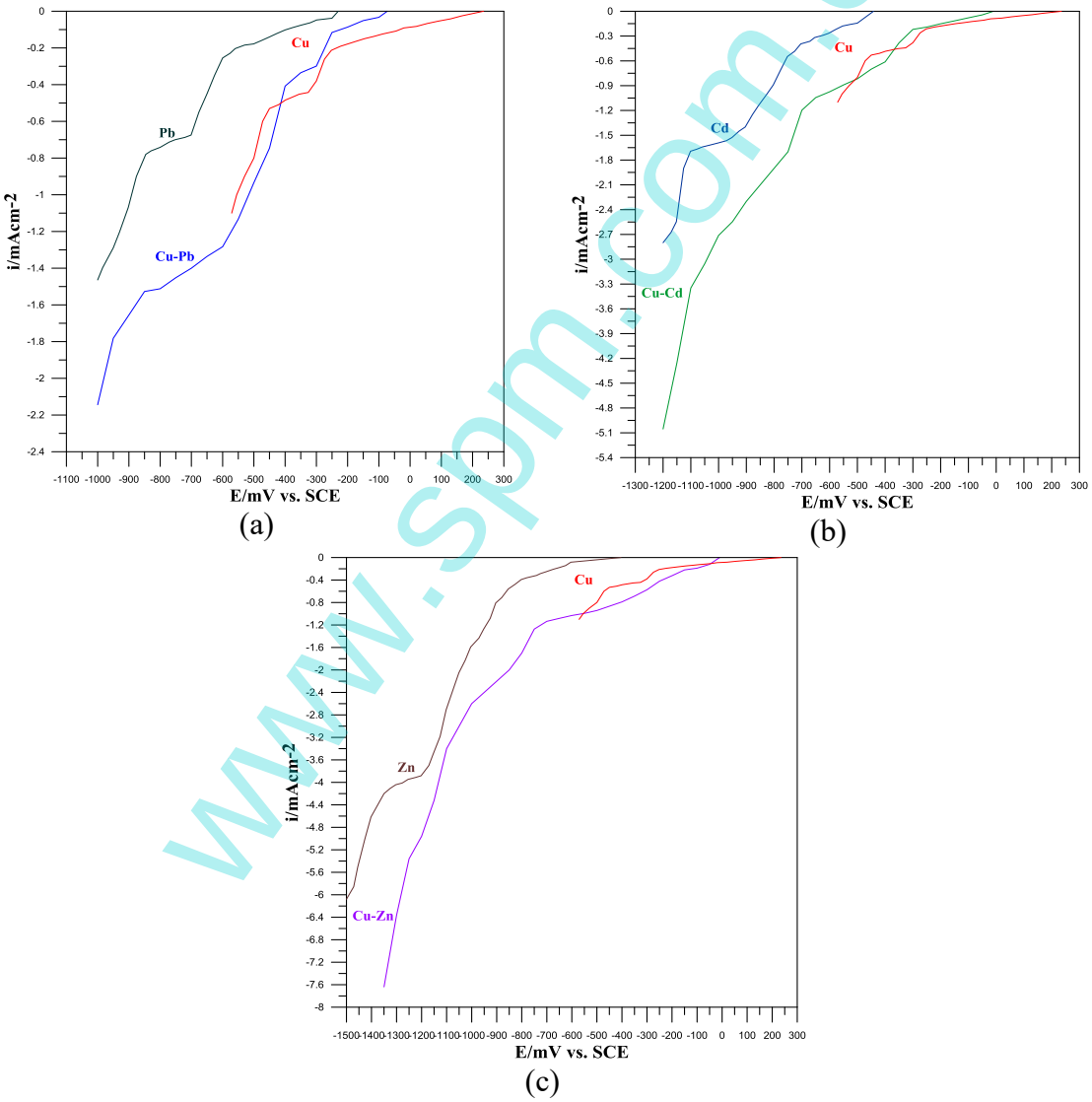

Figure 3. Linear voltammetric curves for reduction of copper-lead (a) copper-cadmium(c) and copper - zinc(d) at stainless steel rotating disc electrode at 1200rpm.in comparison with individual their single metal curves.[Cu]=[Pb]=[Cd]=[Zn]=50 ppm ,supporting electrolyte(0.5 M NaCl+0.1M H_3BO_3), pH=5

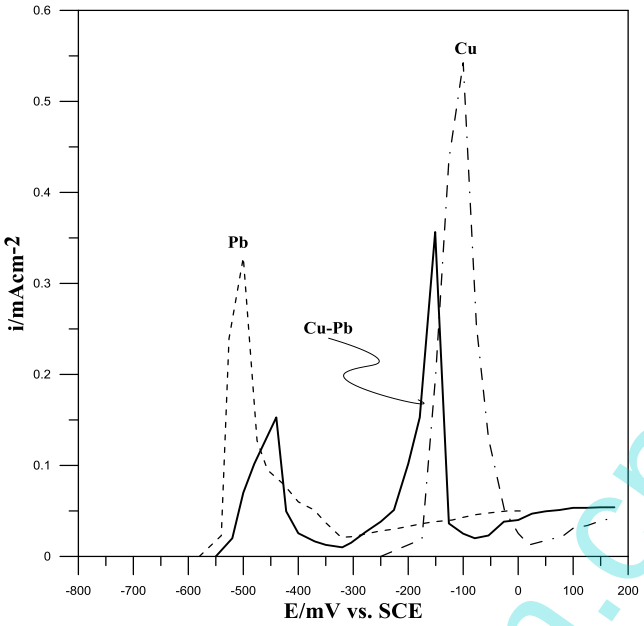

Figure 4. ALSV curves recorded at the sweep rate of $2mVs^{-1}$ for dissolution of Pb, Cu and Cu-Pb binary system. Supporting electrolyte (0.5 M NaCl+0.1M H_3BO_3), pH=5,1200rpm.

Figure 5 shows the phase diagram of Pb-Cu alloy which is eutectic type with no miscibility (solubility) between Pb and Cu in the solid phase [73]. Since the interaction between Pb and Cu in the solid phase is negligible therefor the free energy of each component should not change and the reversible potential of each component in the alloy should be the same as the reversible potential of pure components of the corresponding grain size leading to two separated peaks of dissolution of each component from the alloy. The peak of dissolution of Pb from binary system is shifted to the more positive potential than dissolution of single Pb while that of Cu is shifted to more negative potential than dissolution of single Cu.

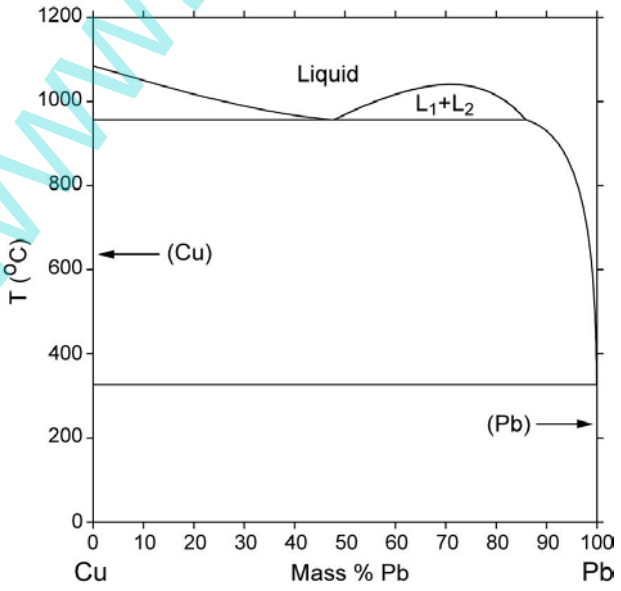

Figure 5 .The phase diagram of Cu-Pb alloy

There is no hump appears at potential more positive than the reversible potential of lead in the dissolution of Cu-Pb binary system from chloride medium in contrast with that appears in the previous work using HBF_4 solution [51]. This may be resulted from the adsorption of Cl^- ions on the surface of the Cu-Pb coating during the dissolution hence preventing formation of such hump.

The ALSV curves of dissolution of single Cd and single Cu and Cu-Cd binary system and the phase diagram of Cd-Cu alloy [73] are shown in Figures (6 and 7) respectively. The ALSVs exhibit three anodic peaks A, B and C .Arguments are found to assign those peaks to the corresponding number of phases in a sequences of Cd, Cu_5Cd_8 and Cu. The Cu_5Cd_8 phase appears when the "current ratio", i.e. the ratio between the employed current density and the diffusion limiting current density of Cu deposition, higher than 3:1as observed in the previous works [52]. In the present work ,the comparison between the current density of electrodeposition of Cu-Cd film at -1025 mV with that of Cu at -380 mV leads to calculate the current ratio to be 4.5:1 which emphases the existing of this phase.Therefore three phases can be existed for Cu-Cd binary system films obtained from diluted chloride solution. Cases are found where the ALSVs point to the existence of all the phases predicted by the phase diagram (Figure 7) in a single alloy deposit. An example of such a case is the deposit of the Cu-Cd alloy obtained by electrodeposition from an electrolyte of the composition 0.01 M $CuSO_4$ + 0.5 M $CdSO_4$ + 0.1 M Na_2SO_4[74]. It is interesting to note that the structure of electrodeposited films from binary systems, as reflected in the ALSV, proved sensitive to both the current ratio and type of substrate used for deposition [53]. In the present work the using of St.St as working electrode may be inhibited the crystallization of $CuCd_3$ which always observed in the ALSVs of Cu-Cd alloy deposited on silver electrode at current ratios 3:1 to 6:1[54].

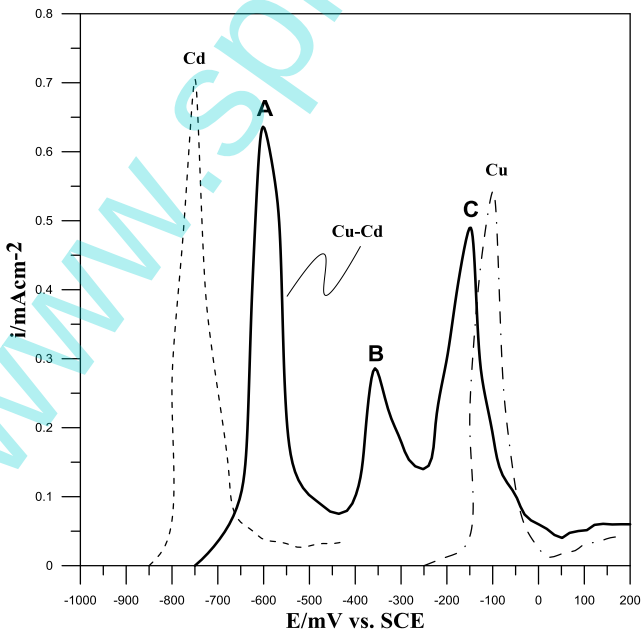

Figure 6. ALSV curves recorded at the sweep rate of $2mVs^{-1}$ for dissolution of Cd, Cu and Cu-Cd binary system Supporting electrolyte (0.5 M NaCl+0.1M H_3BO_3), pH=5,1200rpm.

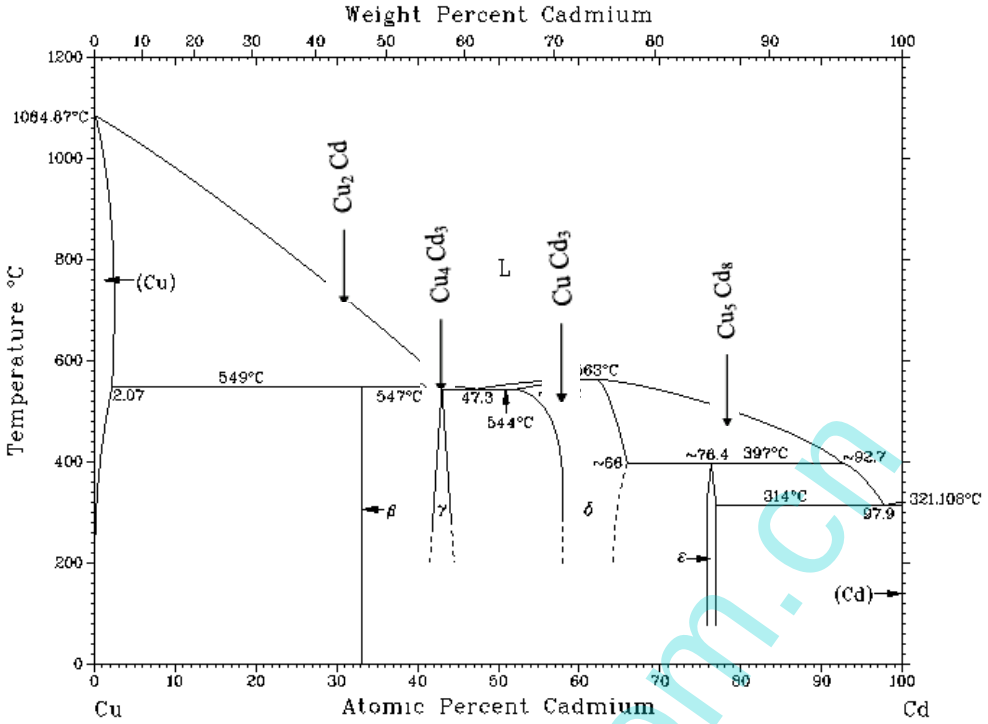

Figure 7. The phase diagram of Cu-Cd alloy

The ALSV curves of dissolution of single Zn, single Cu and Cu-Zn binary system and the phase diagram of Cd-Zn alloy [73] are shown in Figures (8 and 9) respectively. The ALSVs exhibit four anodic peaks A, B, C and D respectively. Peak (A) corresponding to the dissolution of zinc however it is shifted to more positive potential than peak of single zinc dissolution. Peak (B) is found in the region of -700 to -500 mV (SCE) corresponding to the formation of ε-phase .The peak (C) was identified as reflecting the presence of the β-phase [51].The final peak (peak D) represented the dissolution of copper. The present observations is coincided with that of other works [75].

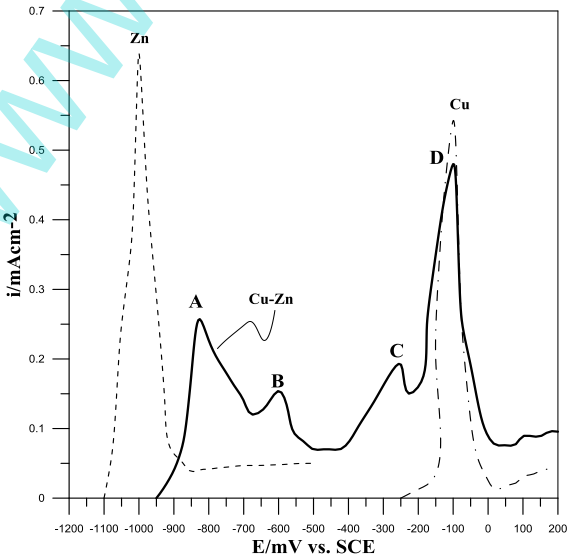

Figure 8. ALSV curves recorded at the sweep rate of $2mVs^{-1}$ for dissolution of Zn, Cu and Cu-Zn binary system. Supporting electrolyte (0.5 M NaCl+0.1M H_3BO_3), pH=5,1200rpm.

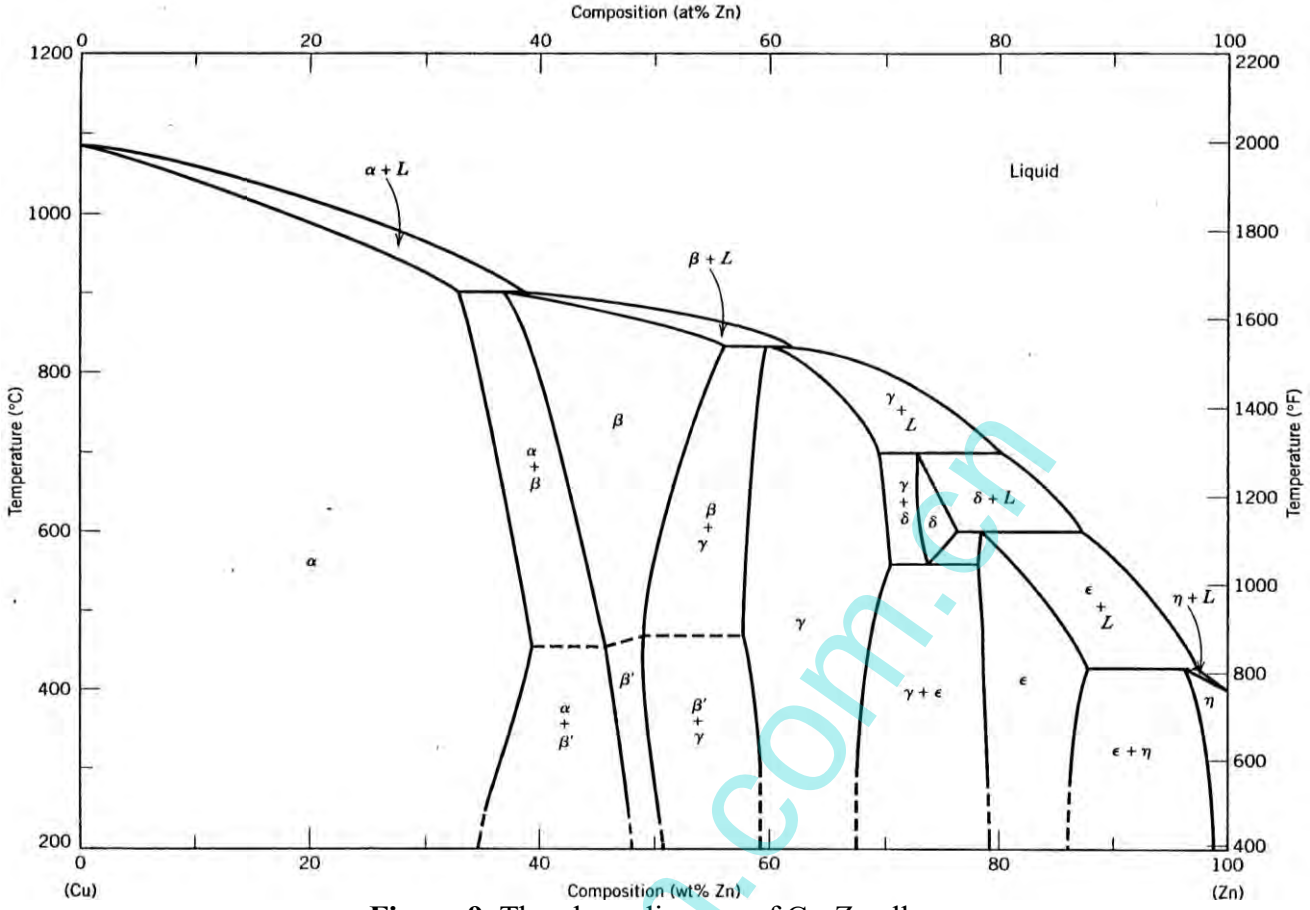

Figure 9. The phase diagram of Cu-Zn alloy

It is cleared that α-phase and η-phase are not found in the Cu-Zn films electrodeposited from chloride medium, in spite of their occurrence in alloys of Cu-Zn electrodeposited from other media such as pyrophosphate [76]. This may interrupted as the effect of the anion on the mechanism of phase formation during the electrolysis. The γ-phase is detected only from metallurgical alloys not electrodeposited alloy.

3.3. Chronoamperometric measurements

Chronoamperometry (CP) was used as an electrochemical technique suitable for electrochemical nucleation mechanisms studies. In chronoamperometry experiments, the potential was stepped from the open-circuit potential to the potential at which the deposition of metal ion would occur. Under these conditions, the system made a transition from no reaction to the steady-state reaction controlled by the rate of mass transfer of metal ions toward the electrode surface [77]. In the case of heterogeneous systems under diffusion control, nuclei formed on the surface contribute to the active surface area available for reaction.

There are several published methods that utilize the coordinates of chronoamperometric peaks to determine nucleation mechanisms and parameters related to nucleation [78], among which the model developed by Scharifker and Hills [79] is the most widely used. This model allows simple and

rapid classification of experimental transients into the two limiting nucleation mechanisms—instantaneous or progressive. Instantaneous nucleation, Eqs. (5 and 6), corresponds to a slow growth of nuclei on a small number of active sites, all activated at the same time, while progressive nucleation, Eqs. (7 and 8), corresponds to fast growth of nuclei on many active sites, activated during the course of electroreduction [80]:

For instantaneous nucleation

$$i = \frac{zF\pi\ (2Dc)^{3/2} M^{1/2} N_0 t^{1/2}}{\rho^{1/2}} \quad (5)$$

$$\frac{i^2}{i_m{}^2} = \frac{1.9542}{\frac{t}{t_m}}\left\{1 - exp\left[-1.2564\left(\frac{t}{t_m}\right)^2\right]\right\}^2 \quad (6)$$

For progressive nucleation

$$i = \frac{2zF\pi\ (2Dc)^{3/2} M^{1/2} AN_0 t^{3/2}}{3\rho^{1/2}} \quad (7)$$

$$\frac{i^2}{i_m{}^2} = \frac{1.2254}{\frac{t}{t_m}}\left\{1 - exp\left[-2.3347\left(\frac{t}{t_m}\right)^2\right]\right\}^2 \quad (8)$$

Where i is the current density(Acm^{-2}), A is the nucleation rate constant(s^{-1}), N_o is the number density of nuclei(cm^{-2}),z ,F ,M ,ρ ,D ,c and t are the number of electron, Faraday constant, the atomic weight, density of the depositing metal(gcm^{-3}),the diffusion coefficient(cm^2s^{-1}),the concentration of the eletrodepositing species ($molcm^{-3}$) and the time of nucleation(s) respectively. i_m and t_m are the current density and the time, as respective peak coordinates. The plots of experimental current transients in $(i/i_m)^2$ versus (t/t_m) coordinates fall at either of these two limiting cases.

The first twenty seconds of current transients recorded at three potential steps for all single and binary heavy metals systems are presented in Figures (10-a,b and 11-a,b) and Figure(12-a-c). Each of the chronoamperograms in these figures were characterized by the initial current increase as a response to the applied potential, formation of a peak characteristic for nucleation, and final convergence to the limiting current corresponding to linear diffusion to a planar electrode. Initial current increase is due to the increase of surface area whenever the nucleation is involved. As nucleation progresses, the nuclei will begin overlapping. Each nucleus will define its own diffusion zone through which metal has to diffuse, representing the mass-supplying mechanism for continuation of growth. Since the diffusion zones are much larger than the underlying nuclei, the overlapping zones would eventually include the entire electrode area. Further reaction is strictly controlled by the rate of mass transfer through the control area of the diffusion zone. Within the diffusion zone, growth of already-established metal nuclei can continue, or additional nucleation can be initiated on various sites, both governed by the steady state conditions [77].The experimental current transients plotted in reduced current–time coordinates, along with the lines for instantaneous and progressive nucleation (solid and dashed lines, respectively described by Eqs. (6 and 8), are shown in Figures (10-c, d and 11-c, d) for single metals and Figure (12-d-f) for binary systems. According to Figure (10-c), the reduced current transients of

copper follow the progressive, nucleation model for all three potential steps in chloride medium using St.St substrate. Copper nucleation mechanisms have been investigated on substrates such as vitreous carbon [77, 81-82], sputtered TiN [83], and copper [84], from solutions containing sulfates [77], pyrophosphate [84], and fluoroborate [83]. Instantaneous copper nucleation mechanisms have been found in each of the cited studies, although inspection of electrode images from the fluoroborate solutions [83] also suggests progressive nucleation mechanisms. In addition, it was found that the type of nucleation mechanism is highly dependent on the solution pH and the type of a supporting electrolyte [77]. The result of the present work reveals the effect of Cl^- ions on the mechanism of nucleation to be switched to progressive nucleation.

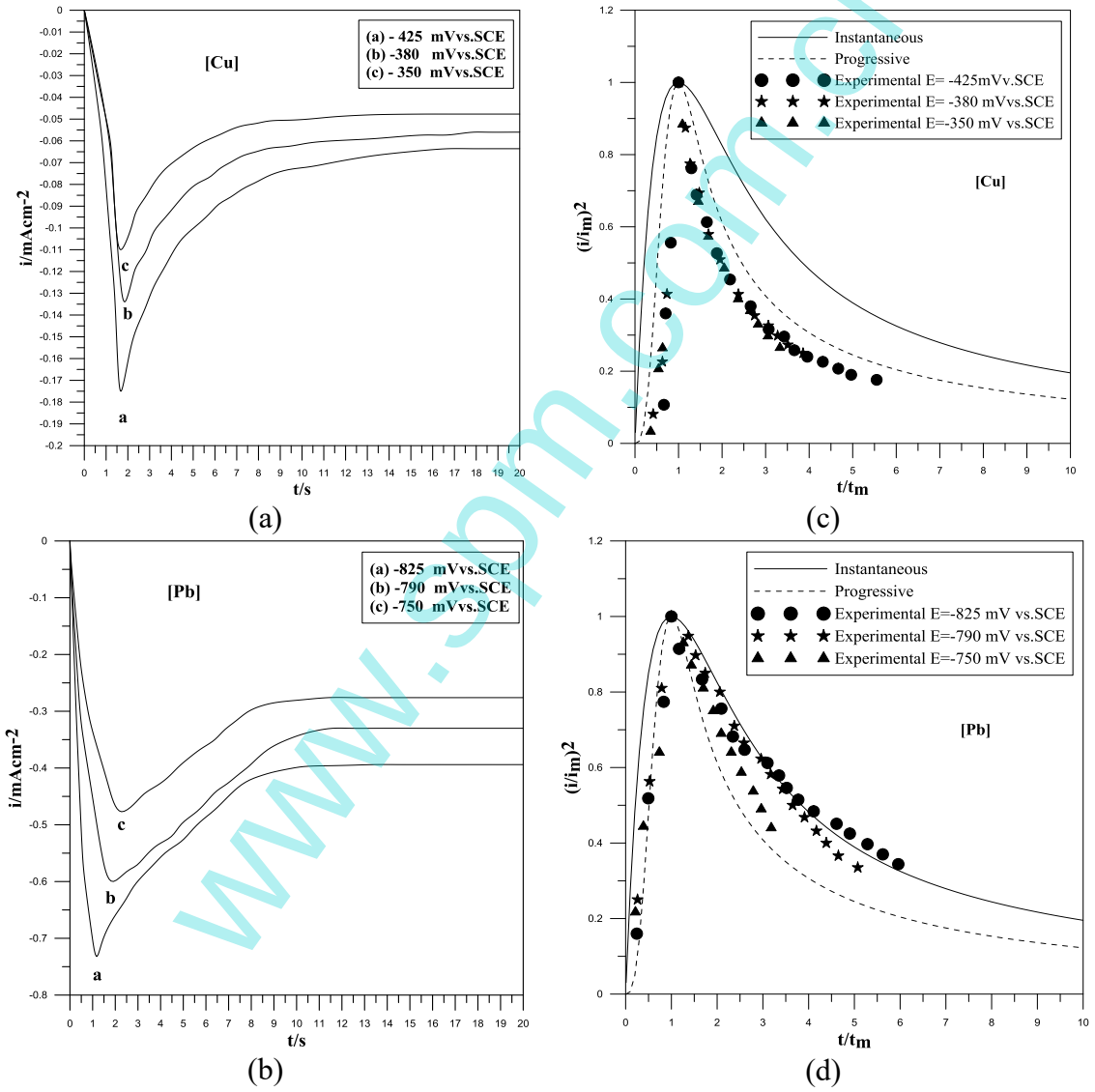

Figure 10. (a-b)Chronoamperometry of Cu and Pb electrodeposition on stainless steel electrode. (c-d)Corresponding Scharifker-Hills' models: [Cu] = [Pb] =50ppm supporting electrolyte (0.5 M NaCl+0.1M H_3BO_3), pH=5.

The reduced current transients of lead follow the instantaneous nucleation model for potential steps equal or higher than -790 mV in chloride medium using St.St substrate as shown in Figure (10-d). At potential step -750 mV, a small deviation from instantaneous model has been observed due to the mixed control of diffusion and charge transfer in this region. However the general behavior is in agreement with previous work using chloride medium at higher concentration of lead [85].

The nucleation mechanism of cadmium is similar to that of copper as shown in Figure (11-c), the nucleation is progressive in chloride medium. The mechanism of Cd electrodeposition has been studied on different metal substrates such as: Cd, Ni, Cu, Se, Pt, glassy carbon, and SnO_2 [86-89]. Observations from cited studies reveal that the growth of Cd crystals has been catalogued as complex due to existence of adsorption and nucleation processes.

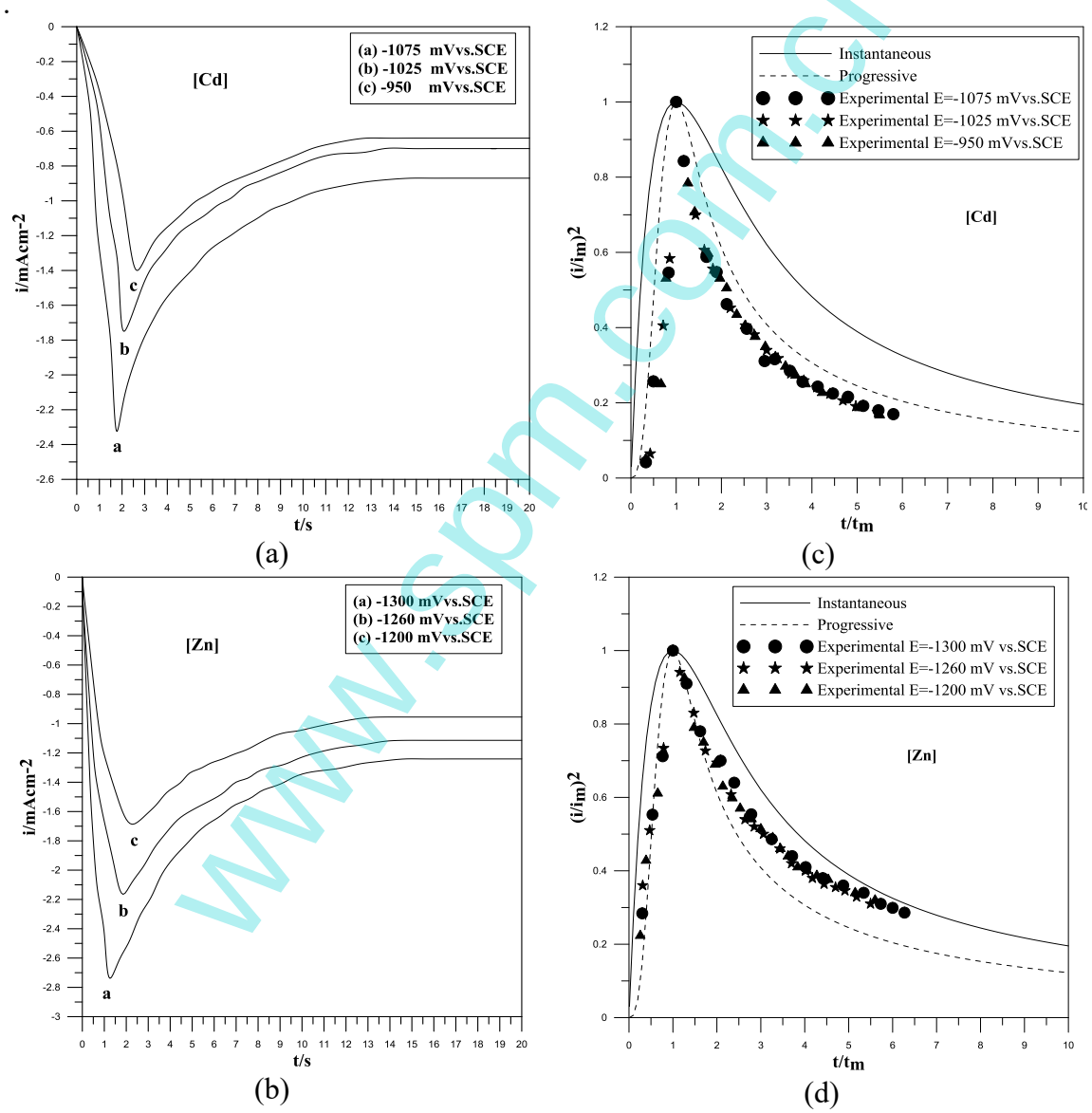

Figure 11. (a-b)Chronoamperometry of Cd and Zn electrodeposition on stainless steel electrode. (c-d)Corresponding Scharifker-Hills' models: [Cd] = [Zn] =50ppm supporting electrolyte (0.5 M NaCl+0.1M H_3BO_3), pH=5.

On the other hand, Gunawardena et al. [86] found that cadmium electrodeposition onto vitreous carbon is progressive in perchlorate and sulfate media while no nucleation occurred in nitrate solution. Recently Edgar et al. [47] studied the electrocrystalization of cadmium on anodically formed titanium oxide using sulfate medium and found that the nucleation process is fitted to progressive model.

According to Figure (11-d), the reduced current transients of zinc follow the progressive at ($t/t_m<4$) then switched to the instantaneous nucleation models at higher values of ($t/t_m>4$) for all three potential steps. Trejo *et al*. [90] found that zinc electrodeposition onto glassy carbon electrode (GCE) changes from instantaneous to progressive with increasing the zinc ions in the bath while the nucleation rate is controlled by transfer charge. Yu *et al*. [91] reported a zinc instantaneous nucleation from acetate baths on GCE with a deviation to progressive nucleation when the potential applied is increased. Sonneveld *et al*. [92] found an instantaneous nucleation with a hemispherical 3D growth on GCE from zincate solutions.

The reduced current transients of Cu-Pb electrodeposition for three potential steps in chloride medium using St.St substrate is shown in Figure (12-d).It is cleared that the transients follow the progressive model. Accordingly it may be concluded that the mechanism of nucleation in the codeposition of lead with copper is controlled by copper which is progressive when copper is alone or mixed with lead. For Cu-Cd system the nucleation process follows the progressive model as shown in Figure (12-e).However the coexistence of two ions will improve the nucleation process to fit the progressive model. The most interesting behavior occurred in Cu-Zn system shown in Figure (12-f). The reduced current transients exhibit progressive nucleation at ($t/t_m<3$) switching to instantaneous nucleation after that which is approximately similar to the nucleation mechanism of zinc alone. Hence the mechanism of nucleation in the codeposition of zinc with copper is controlled by zinc rather than copper. From the above results, it may be concluded that the co-deposition of two metal ions may be led to a dramatic change in the nucleation process which controlled on the rate of the electrochemical reaction during the deposition process of these ions.

3.4. Characterization of the deposits

Figure 13 shows the optical micrographs of the single and binary systems of heavy metals electrodeposited from chloride medium on stainless steel substrate. The electrodeposition have been achieved potentiostatically at cathode potentials -380 mV for Cu,-790 mV for Pb and Cu-Pb, -1025 mV for Cd and Cu-Cd, and -1260 mV for Zn and Cu-Zn systems. The electrodeposition time is 5min, the optical images were taken at 100X magnification. The optical micrograph of stainless steel exhibit smooth surface with some narrow ultrafine grooves resulted from mechanical polishing of this alloy. The optical micrograph of copper shows a bright red color with dendrite structure. From diluted sulfate medium the structure of copper deposited are always dull powdery with big protuberances as found by Bonou et al. [93] in contrast, the present observation reflects the effect of Cl^- on the deposition of copper. The optical images of Pb, Cd and Zn show a dull structures. The optical micrograph of Cu-Pb film shows a new amazing structure which is entirely different from the films of Cu or Pb .

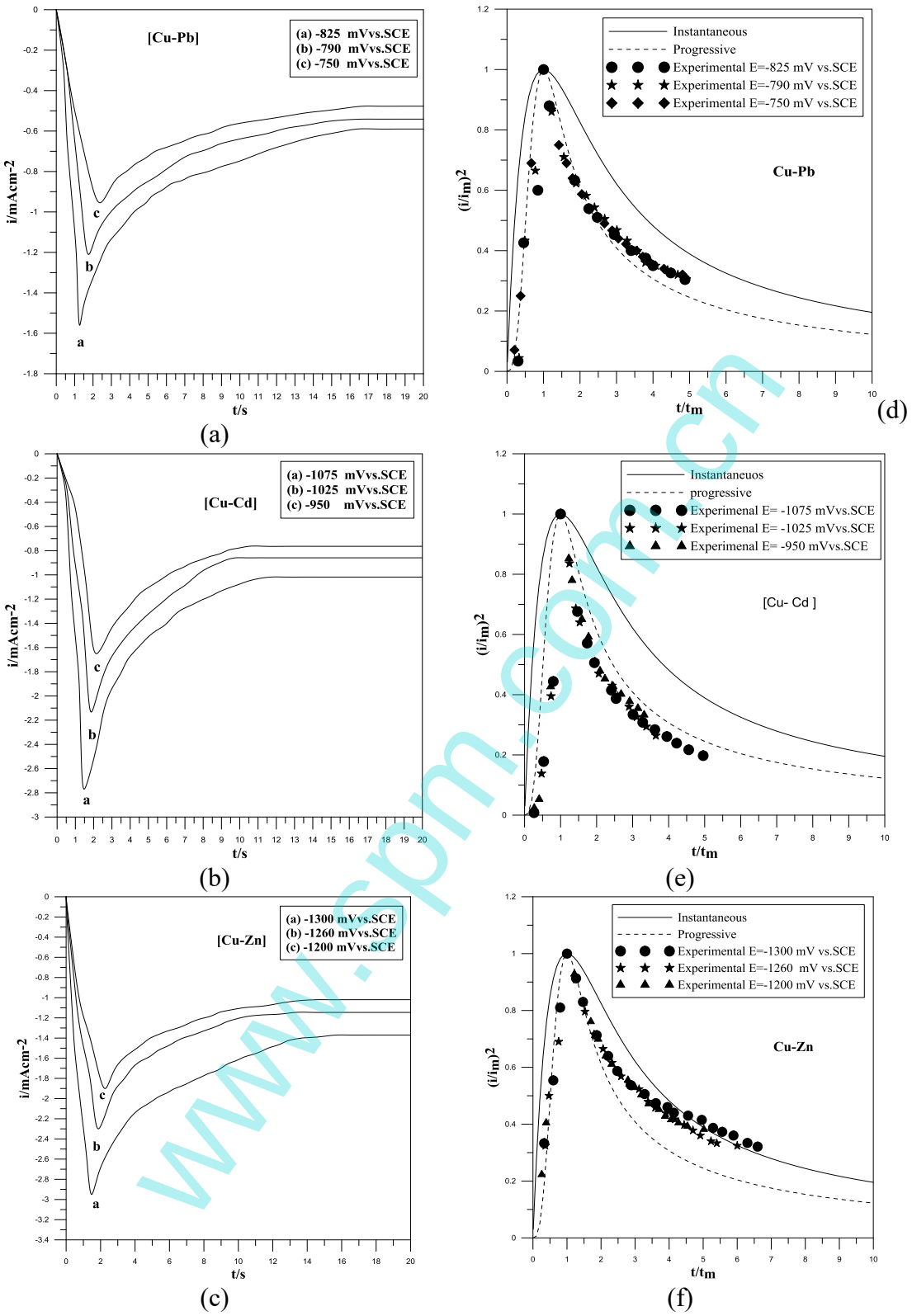

Figure 12. (a-c)Chronoamperometry of Cu-Pb, Cu-Cd and Cu-Zn electrodeposition on stainless steel electrode.(e-f)Corresponding SCHARIFKER-Hills' models: [Cu]=[Pb]=[Cd]=[Zn]=50 ppm supporting electrolyte(0.5 M NaCl+0.1M H_3BO_3),pH=5

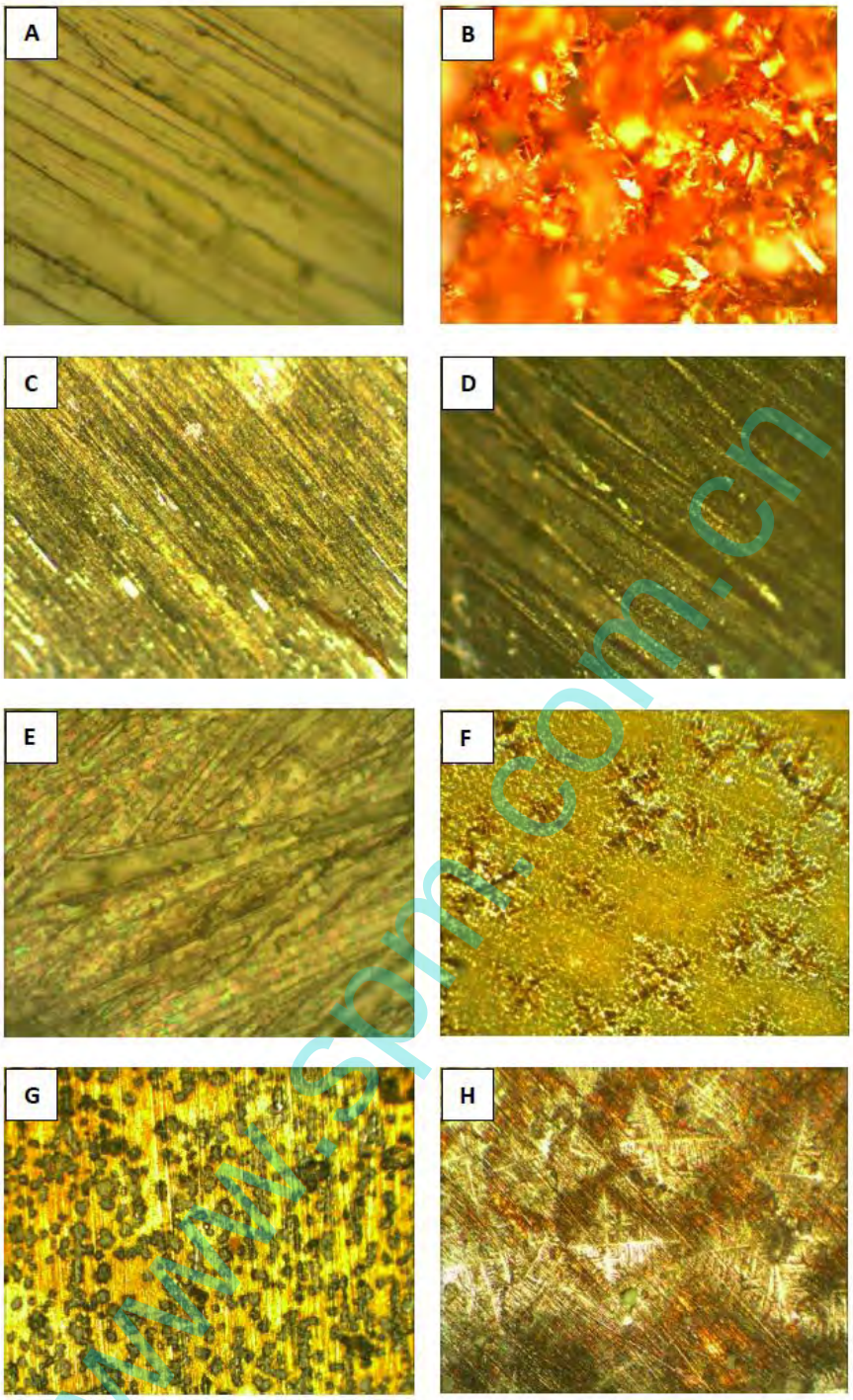

Figure 13. Optical micrographs of cathode substrate and different single and binary heavy metals films electrodeposited at different potentials from chloride medium: A)St.St, B)copper, C)lead, D)cadmium, E)zinc, F)Cu-Pb, G)Cu-Cd, H)Cu-Zn .Magnification ,100X.

This may be attributed to the formation a new phases having different optical properties than single metals. The ALSV profile emphases this observation. Cu-Cd film exhibits another phase structure .From the micrograph of Cu-Cd, it can be seen that the film exhibit the growth of small grains distributed across the surface of film. It also shows uniform surface coverage. The high density of

these grains implies that the nucleation has occurred in all sites. With respect to Cu-Zn film, the optical micrograph gives also a new structure which is entirely different from other binary films and Cu and Pb films .This may be reflected the superimposition of four phases presented in ALSV profile to formulate this film.

Atomic force microscopy (AFM) is an excellent tool to study morphology and texture of diverse surfaces. The knowledge of the surface topography at nanometric resolution made possible to probe thin film surfaces. The versatility of this technique allows meticulous observations and evaluations of the textural and morphological characteristics of the films, showing better facilities than other microscopic methods [94]. Figure14 shows the AFM images for the cathode substrate (St.St) before using, Cu film electrodeposited at electrode potential -380 mV, Pb and Cu-Pb films electrodeposited at electrode potential -790 mV, Cd and Cu-Cd films electrodeposited at electrode potential -1025mV,Zn and Cu-Zn films electrodeposited at electrode potential -1260 mV vs. SCE. Table (1) shows the results of AFM measurements. The most important parameters in AFM measurements are roughness average (Sa), root mean square roughness (Sq), surface skewness (Ssk) and surface kurtosis (Sku).The *roughness average* (*S*a) is the arithmetic average of the absolute values of the measured profile height deviation taken within the sampling length and measured from the graphical center line.

The roughness average can be the same for surfaces with roughness profile totally different because it depends only on the average profile of heights. The *root-mean square roughness* (Sq) is defined as the standard deviation of the surface height profile from the mean height. It is the most commonly reported measurement of surface roughness, and is given by

$$Sq = \left[\frac{1}{N}\sum_{i=1}^{N}(h_i - (h_{av}))^2\right]^{1/2} \quad (9)$$

Where N is the number of pixels in the image (or data points), h_i is the height of the ith pixel, and h_{av} is the mean height of the image. Although the (Sq) evaluations are useful, they provide information only on the height variation, i.e., in the direction perpendicular to the substrate. The (Sq) is more sensitive to peaks and valleys than the average roughness due to the squaring of the amplitude in its calculation. *Skewness* (Ssk) is the third moment of profile amplitude probability density function and is used to measure the profile symmetry about mean line. When the height distribution is symmetrical its value *is* zero. If the height distribution is asymmetrical, and the surface has more peaks than valleys the Skewness moment is positive and if the surface is more planar and valleys are predominant the Skewness is negative. *Kurtosis moment* (Sku) is the fourth moment of profile amplitude probability function and corresponds to a measure of surface sharpness. When (Sku) is 3 indicates a Gaussian amplitude distribution, and the surface is called Mesokurtic, but if Kurtosis is smaller than 3 the surface is flat and called Platykurtic. If the Kurtosis is higher than 3, the surface has more peaks than valleys [95].

The AFM analysis of cathode substrate shows that the root mean square roughness is 0.0589 nm, i.e. the surface of St.St is smooth confirming the mechanical polishing is well. The root-mean square surface roughness values are determined to be 3.12,2.32,and 2.06 nm for Cu, Pb, Cd, and Zn respectively and 3.96,2.62,and 2.16 nm for Cu-Pb, Cu-Cd, and Cu-Zn films receptively.

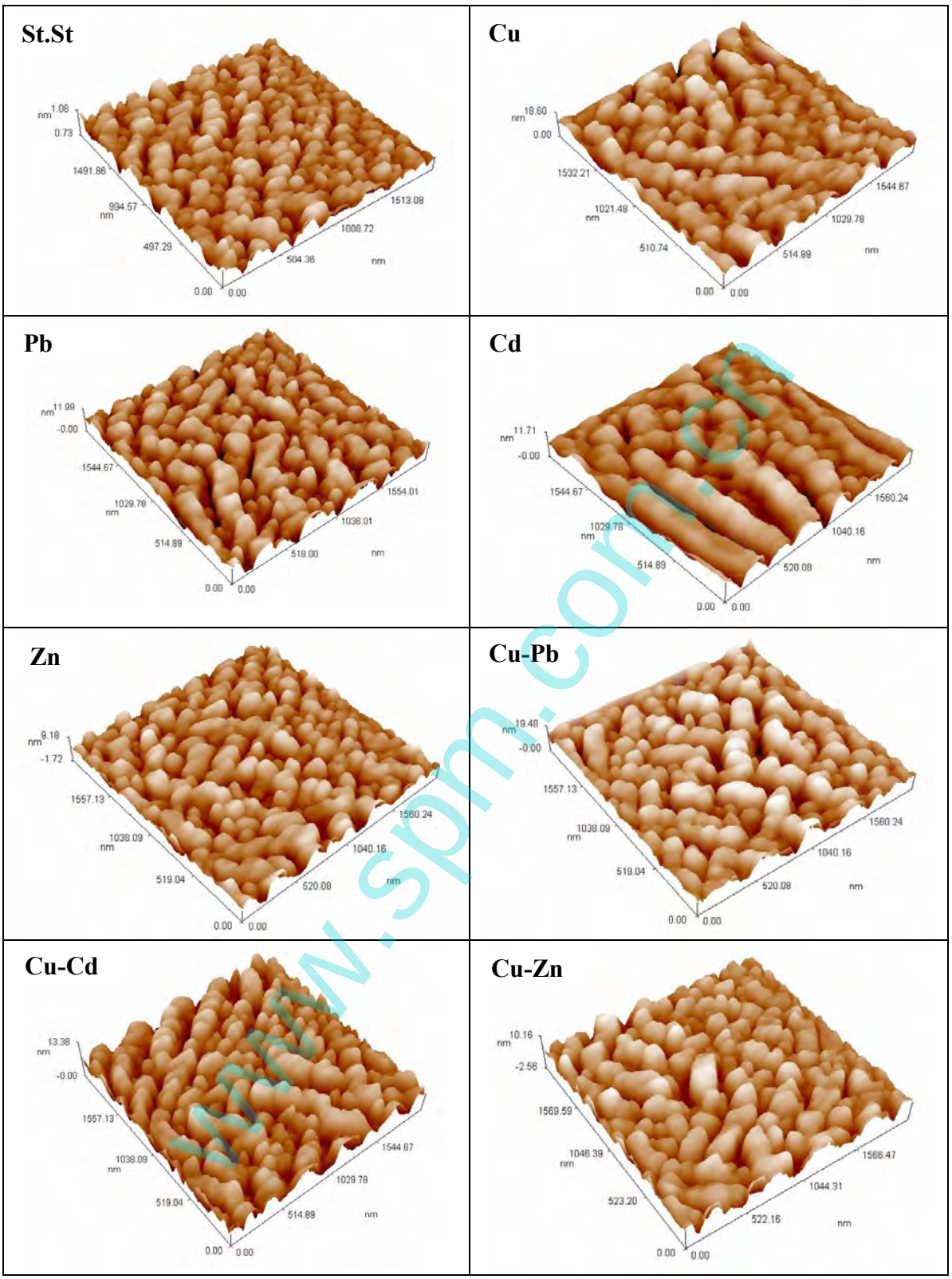

Figure 14. AFM images of st.st substrate and Cu, (Pb, Cu-Pb), (Cd, Cu-Cd), (Zn, Cu-Zn) films electrodeposited potentiostatically at -380mV,-790mV,-1025,-1260 mV vs. SCE from chloride solution respectively.

Table 1. AFM measurements for cathode substrate, single, and binary films electrodeposited potentiostatically at -380mV,-790mV,-1025,-1260 mV vs. SCE from chloride solution respectively.

CSPM Imager surface roughness analysis	St.St substrate	Cu film	Pb film	Cd film	Zn film	Cu-Pb film	Cu-Cd film	Cu-Zn film
⌉Roughness average (sa)[nm]	⌉0.047	2.49	⌉1.9	⌉1.65	⌉1.52	⌉3.2	⌉2.15	1.73
⌉Root mean square (sq)[nm]	⌉0.0589	⌉3.12	⌉2.32	⌉2.06	⌉1.87	⌉3.96	⌉2.62	2.16
⌉Surface skewness (sk)[nm]	⌉-0.666	-0.594	⌉-0.564	⌉-0.669	⌉-0.468	⌉-0.563	⌉-0.605	-0.495
⌉Surface kurtosis (sku)[nm]	⌉3.15	⌉3.16	⌉2.68	⌉3.15	⌉2.63	⌉2.79	⌉2.63	2.76
⌉Peak-peak (sy)[nm]	⌉0.318	⌉18	⌉11.2	⌉10.6	⌉9.09	⌉19.5	⌉12.3	10.2
⌉Ten point height (sz)[nm]	⌉0.194	⌉11.4	⌉6.61	⌉6.33	⌉4.53	⌉12.5	⌉6.9	5.43
Root mean square ⌉slope(sdq)[1/nm]	⌉0.0031	⌉0.130	⌉0.106	⌉0.074	⌉0.0906	⌉0.173	⌉0.119	0.099
⌉Surface area ratio (sdr)	⌉0.0005	⌉0.815	⌉0.558	⌉0.269	⌉0.406	⌉1.41	⌉0.693	0.483
⌉Surface bearing index(sbi)	⌉1.33	⌉1.08	⌉1.38	⌉1.45	⌉1	⌉2.21	⌉1.37	1.08
⌉Core fluid retention index	⌉1.23	⌉1.29	⌉1.24	⌉1.27	⌉1.32	⌉1.28	⌉1.21	1.3
⌉valley fluid retention index	⌉0.149	⌉0.145	⌉0.133	⌉0.145	⌉0.136	⌉0.144	⌉0.134	0.146
⌉Reduced submit height [nm]	⌉0.0302	⌉1.72	⌉0.866	⌉1.01	⌉0.923	⌉1.42	⌉0.827	1.21
⌉Core roughness depth [nm]	⌉0.14	⌉7.59	⌉5.72	⌉4.78	⌉4.6	⌉9.78	⌉6.13	5.51
⌉Reduced valley depth [nm]	⌉0.083	⌉4.31	⌉2.87	⌉2.83	⌉2.29	⌉5.19	⌉3.42	2.89

Accordingly the roughness profile of the single and binary films may be arranged as follows:

For single metals: Cu >Pb>Cd>Zn

For binary system: Cu-Pb>Cu-Cd>Cu-Zn

An important point to be addressed is the influence of nucleation mechanism on the surface roughness of the deposits. It is observed that the roughness is much higher when the initial deposition process is denominated by progressive formation of nuclei. Therefor copper is more roughness than lead and zinc also Cu-Cd film is more roughness than Cu-Zn film because the mechanism of nucleation is progressive. This observation had been confirm by other author [96]. The roughness of cadmium is less than lead in spite of the nucleation process is a progressive type. This may be interrupted as the growth of Cd crystals is controlled by adsorption in combination with nucleation process [88]. The results refer that all films have negative surface skewness which means that surface has more valleys than peaks. Surface kurtosis (sku) for Cu and Cd films are higher than 3while the others are lower than 3 indicating a flat surface (Platykurtic).

4. CONCULUSIONS

Cu-Pb, Cu-Cd, and Cu-Zn films have been successively electrodeposited from simulated chloride solution using St.St cathode under different cathode potentials. Under the studied conditions, the electrodeopsition of the single heavy metals (Cu, Pb, Cd, and Zn) is mass transfer controlled process as revealed by RDE voltammetry. The reduction of copper in the chloride medium follows the

two single step with a well-recognized plateau for the second step Cu(I) to Cu^{o} and no plateau for the first step due to the conditions used in the present work(pH =5,0.5M NaCl ,0.5H_3BO_4,with vigorous agitation).

The LSV curves of electrodeposition of binary metals elucidate the possibility of selective separation of copper from these binary systems since the co-deposition of combined metals start at cathode potential more negative than-500mV vs. SCE. Based on ALSV measurements (number of peaks, their potentials), it is possible to anticipate the phases present in the binary metal films. The peaks of these phases are situated between the dissolution potentials of single metals, their height depends on the potential under which the cathodic co-deposition of the binary system is proceeded.

The results of present research indicate that the nucleation process in the codeposition of two metal ions depends on the interaction between these ions and which of them is controlled on the nucleation process therefore it may be similar or not to the nucleation process of individual ions. Also the Chronoamperometry combined with AFM is a successful experimental approach for characterizing the films deposited electrochemically. Based on the results of CP and AFM, it could be concluded that progressive nucleation always lead to higher roughness of the surface than instantaneous nucleation process.

ACKNOWLEDGEMENT

The authors express their gratitude to Engineering Consulting Bureau/ Al-Qadissya University for financial support of this work under the contract no.28-2.Special thanks is extended to Dr. A. kareem ALSamaraee for his scientific helpful guidance in AFM analysis.

References

1. N.K. Srivastava and C.B. Majumder, *J. Hazard. Mater.* , 151(2008) 8.
2. M.A. Al-Ghouti, M.A.M. Khraisheh and M. Tutuji, *Chem. Eng. J.*, 104 (2004) 83.
3. A.H. Hawari and C.N. Mulligan, *Bioresour. Technol.*, 97 (2006) 692.
4. N. Oyaro, O. Juddy, E.N.M. Murago and E. Gitonga, *Int. J. Food Agric. Environ.*, 5(2007)119.
5. A.T. Paulino, F.A.S. Minasse, M.R. Guilherme, A.V. Reis, E.C. Muniz and J. Nozaki, *J. Colloid Interface Sci.,* 301(2006) 479.
6. R. Naseem and S.S. Tahir, *Water Res.*, 35 (2001)3982.
7. J.P. Chen and X. Wang, *Sep. Purif. Technol.*, 19 (2000) 157.
8. J. Pattanayak, K. Mondal, S. Mathew and S.B. Lalvani, *Carbon*, 38 (2000) 589.
9. G. Naja and B. Volesky, *Colloids Surf.* A, 281 (2006) 194.
10. J.A.S. Tenorio and D.C.R. Espinosa, *Water Manage.* , 21 (2001) 637.
11. S. Kocaoba and G. Akcin, *Desalination*, 180 (2005) 151.
12. M. Mohsen-Nia, P. Montazeri and H. Modarress, *Desalination*, 217 (2007) 276.
13. T. Mohammadi, A. Razmi and M. Sadrzadeh, *Desalination*, 167 (2004) 379.
14. V. Gopal, G.C. April and V.N. Schrodt, *Sep. Purif. Technol.*, 14 (1998) 85.
15. A. Smara, R. Delimi, C. Poinsignon and J. Sandeaux, *Sep. Purif. Technol.*, 44 (2005) 271.
16. S.L. Vasilyuk, T.V. Maltseva and V.N. Belyakov, *Desalination*, 162 (2004) 249.
17. Y.S. Dzyazko and V.N. Belyakov, *Desalination*, 162 (2004) 179.
18. P.B. Spoor, L. Koene, W.R. ter Veen and L.J.J. Janssen, *Chem. Eng. J.*, 85 (2002) 127.

19. C. Ahmed Basha, S. Josephine Selvi, E. Ramasamy and S. Chellammal, *Chem. Eng. J*., 141 (2008) 89.
20. C. Solisio, M. Panizza, P. Paganelli and G. Cerisola, *Resour. Conserv. Recycl*., 26 (1999) 115.
21. J.C. Bazan and J.M. Bisang, *J. Appl. Electrochem*. , 34 (2004) 501.
22. C. Ahmed Basha, N.S. Bhadrinarayana, N.K.M. Anantharaman and K.M. Meera Sheriffa Begum, *J. Hazard. Mater.* , 152 (2008) 71.
23. C. Ahmed Basha, K. Ramanathan, R. Rajkumar, M. Mahalakshmi and P. Senthil Kumar, *Ind. Eng. Chem. Res.* ,47 (2008) 2279.
24. G. Chen, *Sep. Purif. Technol*., 38 (2004) 11.
25. R. Bertazzoli, R. C. Widner, M. R. V. Lanza, R. A. Di Iglia and M. F. B. Sousa,*J. Braz. Chem. Soc*.,8 (1997) 487.
26. R. C. Widner, M. F. B. Sousa and R. Bertazzoli, *J. Appl. Electrochem*. , 28(1998)201.
27. G. Carreño, E. Sosa, I. González,C. P. de León, N. Batina and M. T. Oropeza, *Electrochim. Acta*, 44(1999) 2633.
28. M. S. El-Deab M. M. Saleh, B. E. El-Anadouli and B. G. Ateya, *J. Electrochem. Soc*., 146(1999) 208.
29. C. A. R. Ragnini, R. A. Di Iglia, W. Bizzo and R. Bertazzoli, *Water Res.,* 34(2000) 3269.
30. N. P. Brandon, D. Pilone, G. H.Kelsall and Q. Yin, *J. Appl. Electrochem*., 33(2003) 853.
31. C. Y. Cheng, G. H. Kelsall and D. Pilone, *J. Appl. Electrochem*. , 35(2005) 1191.
32. I.C. Agarwal,A.M. Rochon, H.D. Gesser and A.B. Sparling, *Water Res*.,18(1984)227.
33. L. A. D. Barbosa, L. G. S. Sobral and A. J. B. Dutra, *Miner. Eng*., 14(2001) 963.
34. A. E. Elsherief, *Electrochim. Acta*, 48(2003) 2667.
35. L. H. S Gasparotto, N. Bocchi, R. C. Rocha-Filho and S. R. Biaggio, *J. Appl. Electrochem*., 36(2006) 677.
36. L. C. Almeida, L. H. S. Gasparotto, N. Bocchi, R. C. Rocha-Filho and R. S Biaggio, *J. Appl. Electrochem*. , 38(2008)167.
37. L. C. Ferracin, A. E. Chácon-Sanhueza, R. A. Davoglio, L. O .Rocha, D. Jaffeu, A. R. Fontanetti, R. C. Rocha-Filho,S. R. Biaggio and N. Bocchi, *Hydrometallurgy* ,65 (2002) 137.
38. L. A. M. Ruotolo and J. C Gubulin, *Chem. Eng. J*., 149 (2009) 334.
39. A. H. Sulaymon, A.O. Sharif, T. K. Al-Shalchi and A. H. Abbar , *Journal of Chemical Science and Technology* , 2 (2013) 175.
40. E. Budevski,G. Staikov and W. J. Lorenz, *Electrochim. Acta*, 45(2000)2559.
41. A. Milchev and L .Heerman, *Electrochim. Acta*, 48(2003)2903.
42. M. Gu and Q. zhong, *J. Appl. Electrochem*. , 41 (2011) 765.
43. D. Grujicic and B. Pesic, *Electrochim. Acta* 50(2005)4426.
44. D.Grujicic and B.Pesic, *Electrochim. Acta* 47(2002)2901.
45. F. Nasirpouri, *ionics*, 17 (2011)331.
46. M. Gircis and E. Ghali, *J.Appl.Electrochem*, 17 (1987)1234.
47. J.E. Carrera-Crespo,P. Acevedo-Pena, M. Miranda-Herandez and I. Gonzalez, *J. Solid State Electrochem*,17 (2013) 445.
48. T. Montiel, O. Solorza and H. Sanchez, *J. Electrochem. Soc*., 147 (2000) 1031.
49. Q. Zhang and Y. Hua, *J. Appl. Electrochem*, 41 (2011) 705.
50. Y. Mo, Q.Huang,W.Li,S. Hu, M. Huang and Y.Huang, *J.Appl.Electrochem*41(2011),859.
51. V. D. Jovic, R. M. Zejnilovic, A.R. Despic and J.S. Stevonic ,*J.Appl.Electrochem*, 18 (1988)511.
52. J.S.Stevonic , A.R.Despic and V.D.Jovic, *Electrochim. Acta*, 42(1997)873.
53. V.D. Jovic, A.R. Despic, J.S. Stevonic and S.Spaic, *Electrochim. Acta*, 34(1989)1093.
54. J.S. Stevonic , V.D. Jovic and A.R. Despic ,*J.Electroanal.Chem*.,349(1993) 365.
55. M.R.H. deAlmeida, E.P. Barbano, M.F. deCarvalho, I.A. Carlos, J.L.P. Siqueira and L.L. Barbosa, *Surface & coatings Technology*,206 (2011) 95.
56. F.L. G.Silsva, D.C.B. doLago, E.D. Elia and L.F. Senna, *J.Appl.Electrochem*, 40 (2010) 2013.

57. R. Juskenas,V. Karpaviciene,V. Pakstas,A. Selskis andV.Kapocius, *J. Electroanal. Chem*., 602(2007)237.
58. S.D. Beattie and J.R. Dahn, *J. Electrochem. Soc*. 150(2003) C802.
59. L.F. Senna,S.L. Diaz and L. Sathler, *J.Appl.Electrochem*,33 (2003) 1155.
60. E.C. Weakly and H. Dicamillo, Patent US 99-248064(RRT 10 Box 480, Glenwood, NM 88039, (2001).
61. D. Barnes and T.R. Raponi, *Miner. Metall. Process*. , 8 (1991) 128.
62. M. Paidar, K. Bouzek, M. Laurich and J. Thonstad, *Water Environ. Res*., 72 (2000) 618.
63. C. P. De Leon and D. Pletcher, *Electrochim. Acta*, 41 (1996), 533.
64. C. Ponce de Leon and F.C. Walsh ,*Trans Inst Met Fin* ,81(2003)B9.
65. C. Nila and I. Gonzalez, *J. Electroanal. Chem*., 401 (1996) 171.
66. J. Crousier and I. Bimaghra, *Electrochim. Acta*, 34(1989)1205.
67. C. Karwas and T. Heped, *J. Electrochem. Soc*, 136 (1989) 1672.
68. B.V. Tilak, A.S. Gendron and M.A. Mosoiu, *J. Appl. Electrochem* ,7 (1977)495.
69. A.J. Bard and L.R. Faulkner, Electrochemical methods: fundamentals and applications, Wiley, New York (2001).
70. D.R .Gabe and P.A .Makanjuola, In: Electrochemical engineering. IChemE symposium series, 98(1986) 309.
71. A.R. Despic,V.d. Jovic,in P.R.E. White, J.O.M. Bockreis and B.E. Conway(Eds.), Modern Aspects of Electrochemistry, Plenum Press., New York,(1995)143.
72. B.M. Jovic,Ts. Dobrovolska,U. Lacnjevac,I. Krastev and V.D.J ovic, *Electrochim. Acta*, 54(2009)7565.
73. M. Hansen and K. Andrenko, 'Constitution of Binary Alloys', McGraw-Hill, New York, Toronto, London (1958).
74. V.D. Jovic,S. Spaic,A.R. Despic, J.S. Stevanovic and M. Pristavec ,*Materials Science and Technology*, 7(1991)1021.
75. J. Stevanovic, L. J. Skibina, M. Stefanovic, A. Despic and V. D. Jovic, *J. Appl. Electrochem*, 22 (1992) 172.
76. V.V. Bondar,V.V. Grimina and V.N. Paviov, Itagi nauki I techniki, *Electrokhimiya* 16, (1980).
77. D. Grujicic and B. Pesic, *Electrochim. Acta*, 47(2002)2901.
78. M.E. Hyde and R.G. Compton, *J. Electronal. Chem*., 549 (2003) 1.
79. B. Scharifker and G. Hills, *Electrochim. Acta* ,28 (1983) 879.
80. M.P. Pardave, M.T. Ramirez, I. Gonzales, A. Serruya and B.R. Scharifker, *J. Electrochem. Soc*., 143 (1996) 1551.
81. A.I. Danilov, E.B. Molodokina and Yu. M. Polukarov, *Russ. J. Electrochem*. , 38(2002) 732.
82. A.I. Danilov, E.B. Molodokina, A.A. Baitov, I.V. Pobelov and Yu.M. Polukarov, *Russ. J. Electrochem*. , 38 (2002) 836.
83. G. Oskam, P.M. Vereecken and P.C. Searson, *J. Electrochem. Soc*., 146 (1999) 1436.
84. A. Radisic, J.G. Long, P.M. Hoffmann and P.C. Searson, *J. Electrochem. Soc*., 148 (2001) C41.
85. M.Gircis and E.Ghali, *J.Appl.Electrochem*, 17 (1987), 1234.
86. G. Gunawardena, G. Hills and I. Montenegro, *J. Electronal. Chem*., 184 (1985) 371.
87. R. Barnard, G. S. Edwards, J. Holloway and F.L. Tye, *J.Appl.Electrochem*, 13(1983)751.
88. A.M. AbedEl-Halim, *J.Appl.Electrochem*, 14 (1984) 587.
89. T. Montiel,O. Solorza and H. Sanches, *J. Electrochem. Soc*., 147 (2000) 131.
90. G. Trejo, R. Ortega, Y. Meas, P. Ozil, E. Chainet, B. Nguyen, *J. Electrochem. Soc*., 145 (1998)4090.
91. J. Yu, H. Cao, Y. Chen, L. Kang and H. Yang, *J. Electroanal. Chem*., 474(1999) 69.
92. J. Torrent-Burgue and E. Guaus, *J. Appl. Electrochem., 37(*2007) 643.
93. L. Bonou,M. Eyraud,R. Denoyel and Y. Massiani, *Electrochim. Acta*, 47(2002)4139.
94. B.R. Kumar and T.S. Rao,digest ,*Journal of nanomerials and biostructures*,7(2012)1881.

95. S. N. Magonov, M.-H. Whangbo, Surface Analysis with STM and AFM, VCH Publishers, Inc., New York (1996).
96. M.L. Mnford, M.L. Sartorelli, L. Seligman, and A.A. Pasa, *J. Electrochem. Soc.*, 149(2002) C274